Direct Threat of a UV-Ozone Treated Indium-Tin-Oxide Substrate to the Stabilities of Common Organic Semiconductors

Ming-Fai Lo, Tsz-Wai Ng, Hin-Wai Mo, and Chun-Sing Lee**

Ultraviolet-ozone treated indium-tin-oxide (UV-ITO) glass substrates have been widely and unquestioningly used in the field of organic electronics to improve both device performance and stability. Evidence is presented here for rapid decay of common organic films such as *N*,*N*′-bis(naphthalen-1-yl)-*N*,*N*′-bis(phenyl)-benzidine (NPB), tris(8-hydroxy-quinolinato)aluminum (Alq_3), and rubrene when they are in contact with an UV-ITO substrate. While the photoluminescence (PL) of these organic films deposited on an UV-ITO substrate decay rapidly under illumination; those on quartz substrates are comparatively much more stable. Results from X-ray and UV photoemission spectroscopies (XPS and UPS) further suggest that degradations of the rubrene films on UV-ITO substrate are mainly attributed to active oxygen species generated upon UV-ozone treatment. These reactive oxygen species on the UV-ITO surface behave as a reservoir of oxygen that interacts with rubrene and shifts its highest occupied molecular orbital (HOMO) level away from the Fermi level. This interaction induces a gap-state in the energy gap of rubrene, which acts as a charge recombination center. More importantly, enhanced stabilities of rubrene-based organic photovoltaic (OPV) devices are demonstrated when they are fabricated on gold-coated or trifluoromethane (CHF_3) plasma-treated ITO. The presented works shows that the commonly used UV-ITO substrate is a threat to the stability of addlayer organic semiconducting films.

1. Introduction

Indium tin oxide (ITO) is the most commonly used transparent electrode in organic-light emitting devices (OLEDs) and organic photovoltaic (OPV) devices in both academics and industry.[1–7] Early studies have been concerned with the possible damaging effects of indium diffusion from ITO into the organic layers.[8–12] However, Lee et al. later reported that indium diffusion is not obvious before prolong operation (>2000 h)[8] and ITO is therefore used extensively with little alert.[6–14]

Dr. M.-F. Lo, Dr. T.-W. Ng, H.-W. Mo, Prof. C.-S. Lee
Center of Super-Diamond and Advanced Films (COSDAF)
Department of Physics and Materials Science
City University of Hong Kong
Hong Kong SAR, P. R. China
E-mail: tszwaing@cityu.edu.hk; apcslee@cityu.edu.hk

DOI: 10.1002/adfm.201202120

Over the past two decades, many surface modification techniques of ITO substrates have been developed for enhancing performance and stability of organic electronic devices.[13–17] Among those surface-modifying methods, UV-ozone and oxygen plasma are well-recognized as the standard treatment for ITO substrates for enhancing the work function of ITO via increasing the surface oxygen content.[13,17,18] However, the effects of such treatments decrease over time.[19–21] Subsequent decrease in work functions over time is considered to cause carriers unbalance and thus affect the device reliability.[10,19,22] Recently, our studies hint that oxygen radicals generated upon UV-ozone treatment may be another cause for degradation of the fullerene (C_{60}) layer in a standard copper phthalocyanine (CuPc)/C_{60} OPV devices fabricated on an ITO substrate.[23] Indeed, C_{60} has been shown to be particularly sensitive to oxygen;[24,25] its degradation caused by the oxygen radical generated is expected.

To date, the implication and possible threats of ITO to other common organic materials have not been systematically investigated. Here, we study the effects of ITO substrates on the stability of three commonly used organic semiconductors, namely *N*,*N*′-bis(naphthalen-1-yl)-*N*,*N*′-bis(phenyl)-benzidine (NPB), tris(8-hydroxy-quinolinato)aluminum (Alq_3), and rubrene. While mild decay is observed in the PLs of all three materials upon contact with as-cleaned ITO (AC-ITO), the degradation is rapid when the same films are deposited on ultraviolet-ozone treated indium-tin-oxide (UV-ITO). The effects of UV-ITO on degradation of rubrene were further investigated using ultraviolet photoelectron spectroscopy (UPS) and X-ray photoelectron spectroscopy (XPS). To further consolidate our discussions, rubrene/C_{60} OPV devices are fabricated on UV-ITO substrate and gold-coated/CHF_3 plasma-treated ITO substrates. Contrasting comparison in device stabilities confirms that the degradation in organic film/device performance is correlated to the treatment in prior to organic film deposition. The presented works indicates that most widely used ITO substrates and the UV-ozone treatments indeed cause a potential threat to the stability of many common organic semiconducting films.

2. Results and Discussions

2.1. PL Quenching of Organic Materials on Different Substrates

Figure 1a compares photoluminescence (PL) spectra of 50 nm NPB, Alq_3 and rubrene films deposited on quartz, AC-ITO and UV-ITO glass substrates before (black solid line) and after (symbol) 40 min of 1.5G 1 Sun illumination. PL deterioration can be clearly observed in all films upon illumination. It is interesting to note that the extent of PL deterioration depends on the substrate on which the organic films were prepared. Figure 1b compares the degradation rates of the above film samples. With reported high sensitivities to photo-oxidation of rubrene, we observe an obvious difference in PL characteristics before and after illumination.[26] For rubrene films prepared on quartz and AC-ITO substrates, there is still considerable PL responses (>50%) even after 40 min illumination. However, PL of rubrene prepared on UV-ITO substrates is almost completely quenched over the same illumination time period. The above observations clearly show that the UV-ITO substrate does play an important role in accelerating the rubrene degradation.

To further distinguish the effects of oxygen species from the ITO substrate and those from the atmosphere, a PL degradation experiment was carried out on a specially patterned UV-ITO substrate on which ITO was etched away from the central region marked with a capital letter "A" (**Figure 2**a). A 50 nm rubrene film was deposited onto the substrate (marked with the\lines). The sample was held by a sample holder covering the bottom region (marked with/lines). The sample was then irradiated with 1 Sun

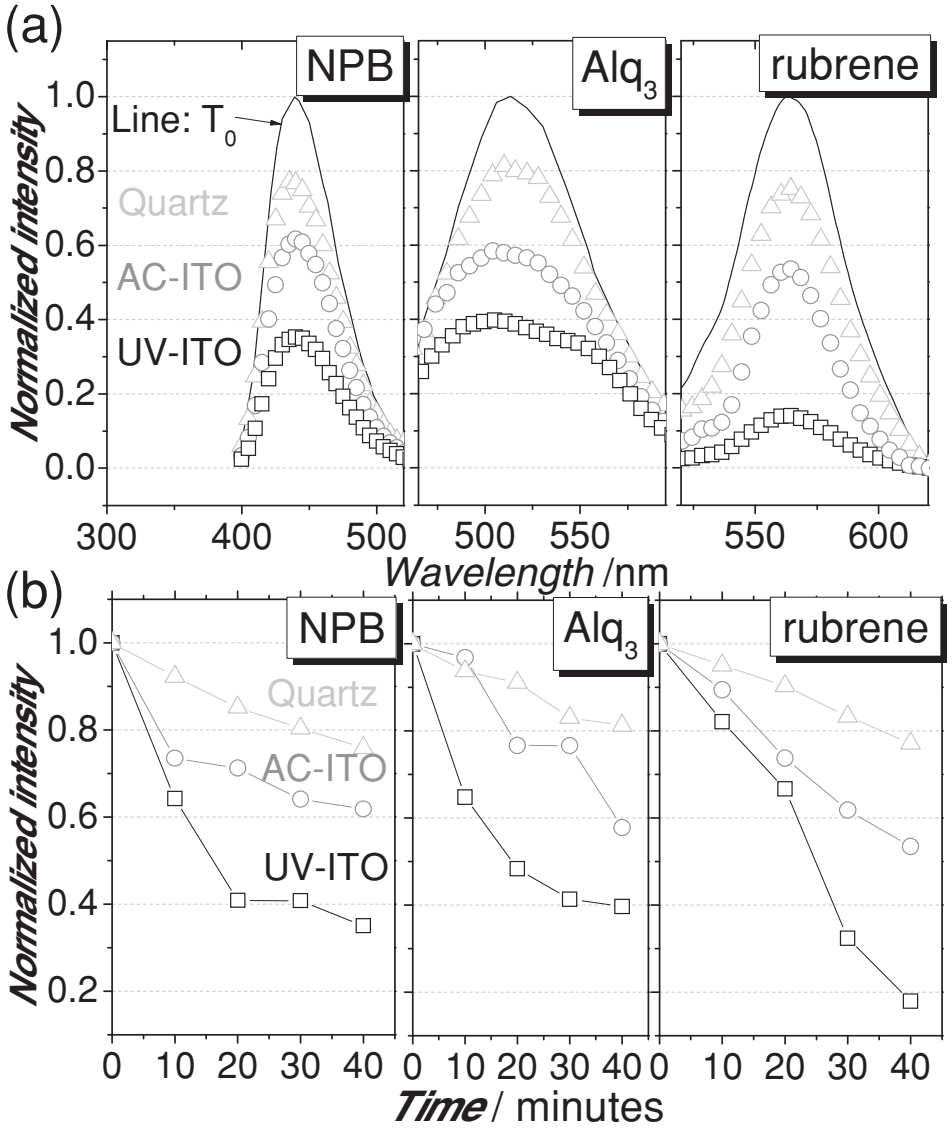

Figure 1. a) PL spectra of NPB, Alq_3, and rubrene films prepared on quartz (△), AC-ITO (○), and UV-ITO (□) substrates. All PL signals are normalized with respect to initial PL intensity. The solid line shows the initial PL signal measured at room condition (T_0) while the symbols shows the PL signal after 40 min illumination under 1 Sun ($T_{40,1sun}$). b) PL deterioration in NPB, Alq_3, and rubrene films prepared on quartz (△), AC-ITO (○), and UV-ITO (□) substrates over continuously illumination for 40 min under 1 Sun.

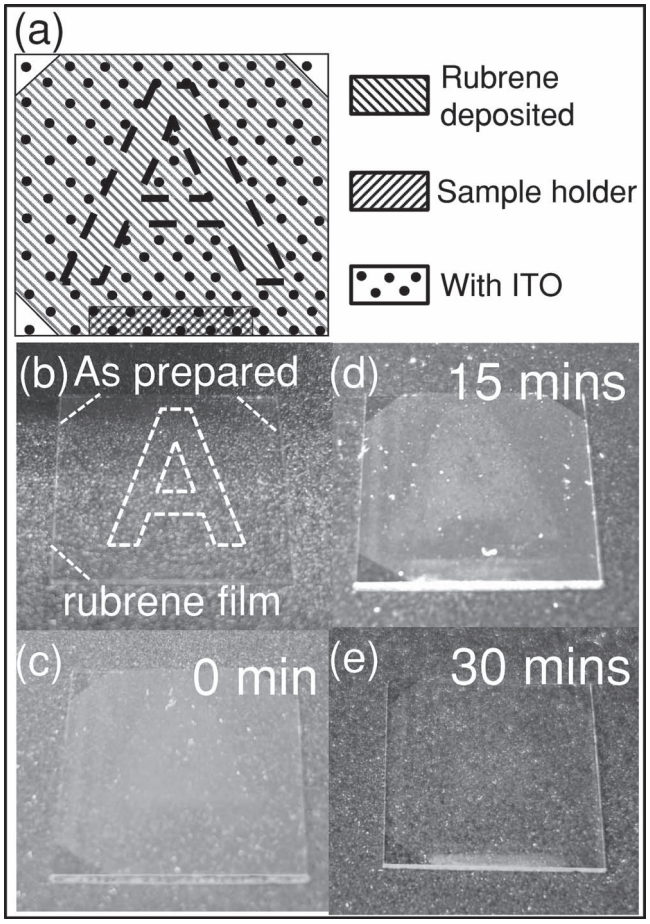

Figure 2. a) Schematic diagram of a patterned UV-ITO substrate. The area inside the letter A is ITO-free. Photographs of as-prepared rubrene sample taken under b) normal-light and c) UV-illuminated conditions. Photographs of rubrene coated sample taken under UV illuminated condition after d) 15 min and e) 30 min irradiation under 1 Sun.

AM1.5G illumination for 0, 15, and 30 min. It can be seen from Figure 2c that the rubrene film shows uniform PL before illumination. After 15 min of illumination, the region of rubrene in contact with ITO (region marked with •, i.e., outside the A mark) shows much weaker PL intensity than the region without ITO (A). It is interesting that the region covered by the sample holder (bottom rectangular region) shows the highest PL intensity. After 30 min of illumination, PL from the rubrene region in contact with ITO can hardly be observed, while the sample-holder-covered region still shows a relatively strong PL (Figure 2e). These results suggested that both the ITO substrate and the simulated solar illumination accelerate degradation of the rubrene film.

We further examine the effect of substrate on the PL degradation of NPB and Alq_3. It can be seen from Figure 1 that both of these materials show similar PL degradation on UV-ITO substrates. These verify that the most widely used UV-ITO substrate can in fact causes obvious stability problems to common organic semiconductors. Degradation mechanisms caused by the UV-ITO substrate were further studied using XPS and UPS analysis.

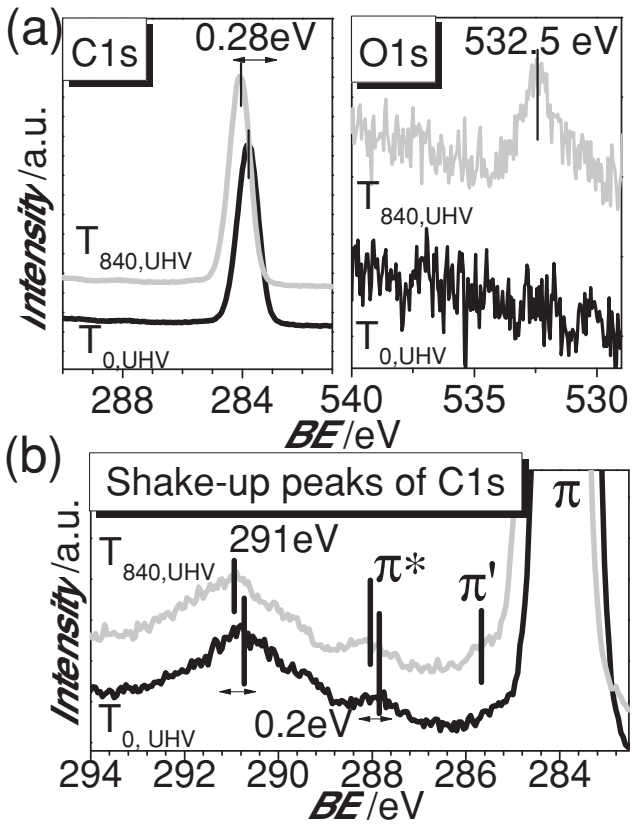

Figure 3. XPS core level spectra of a) C1s and O1s of rubrene film prepared on UV-ITO substrate at $T_{0,UHV}$ and $T_{840,UHV}$. b) Enlarged shake-up peaks of C1s at $T_{0,UHV}$ and $T_{840,UHV}$.

2.2. XPS Studies of Rubrene Degradation on UV-ITO Substrates

To probe the implications of UV-ITO on an addlayer organic film, a 5 nm rubrene film was thermally evaporated onto a UV-ITO substrate in an ultrahigh vacuum (UHV) of 10^{-9} Torr and transferred without breaking the vacuum to an analysis chamber for photoemission studies.

Figure 3a compares the C1s and O1s core levels peaks of a freshly prepared rubrene film measured under UHV without (T_0) and after storage of 840 min in UHV ($T_{840,UHV}$) (different ageing condition are hereafter referred as $T_{time,\ condition}$). The pristine rubrene ($C_{42}H_{28}$) film shows only a single C peak at ≈284 eV (no O1s peak) during initial measurements. After 840 min aging in UHV, the C peak of rubrene shows an obvious shift towards a higher binding energy (BE) by 0.28 eV and a small O peak at ≈532.5 eV emerges. Direction of the C1s peak shift suggests possible oxidation of rubrene to form a rubrene$^{\delta+}$-$O_x^{\delta-}$ complex.

It might be doubtful whether the changes in Figure 3a are caused by residual oxygen in the testing UHV analysis chamber. To rule out this possibility, the same experiment was repeated by depositing rubrene on a sputter-cleaned Au substrate. The corresponding XPS spectra are shown in Figure S1 in the Supporting Information. Negligible shift in C1s peak and absence of O1s peak after the same aging duration confirm that the oxygen peak emergence and the C peak shift in Figure 3a are not due to environmental oxygen in the UHV analysis chamber. We can

thus reasonably attribute those observations to the oxygen specious from the UV-ITO substrate.

The chemical interaction between UV-ITO and rubrene also induces changes in electronic structures in the rubrene film. Figure 3b shows a magnified portion of Figure 3a from 294 to 283 eV. The broad peaks found at ≈291 eV are shake-up peaks commonly observed in molecules with aromatic structures. The peaks found at around 288 eV corresponds to shake-up peaks depicting the π–π* transition of rubrene. The closest peak labeled π* (≈288 eV) near the main peak π (≈284 eV) carries information revealing the rough position of the lowest unoccupied molecular orbital (LUMO) of the testing material.[27] Upon 840 min aging in UHV, both the mentioned peak at 288 and 291 eV were shifted towards the higher BE by ≈0.2 eV. Meanwhile, there is a new gap state peak marked π' emerges near the main peak at 285.7 eV. Emergence of this new peak is probably due to an oxygen-induced gap state within the forbidden energy gap of rubrene. The XPS results suggest that the UV-ITO substrate can indeed change the electronic structures of rubrene upon aging.

2.3. Valence Feature Changes of Rubrene During Degradation on Different Substrates

To understand the changes in the valence electronic structures and charge transporting properties of the organic film induced by the UV-ITO substrate, aging of rubrene films in UHV was studied with UPS. **Figure 4**a shows UPS spectra of rubrene deposited on UV-ITO substrates before (solid line) and after (dash-dotted line) timed aging in UHV. The experiment was also repeated using a sputtered Au substrate and a UV-ITO substrate further treated with CHF_3 plasma (CHF-ITO). **Table 1** summarize the information obtained from the UPS studies including the work functions and the highest occupied molecular orbital (HOMO) energies of rubrene prepared on the various substrates. All the reported values are relative to the Fermi levels. Figure 4b illustrates the HOMO level shift of rubrene films prepared on various substrates including UV-ITO, Au, and CHF-ITO for 840 min. It is noted that for rubrene film prepared on UV-ITO substrate, the HOMO level gradually shifts away from the Fermi level by more than 0.2 eV. However, the same films prepared on Au and CHF-ITO substrates show stable valance electronic and chemical structures over the 840 min aging.

All the above photoemission results ascertain that UV-ITO behaves as an intrinsic oxygen reservoir for oxidation of rubrene. The surface oxygen induced during UV-ozone treatment of ITO substrate acts as an active reactant that initiates and accelerates the film degradation. Direct interaction between the surface reactive oxygen and rubrene results in rubrene$^{\delta+}$-$O_x^{\delta-}$ formation and seriously affects the valence electronic structures of rubrene films. The above observations have far-reaching implications in device degradation, suggesting elimination or isolation of the UV-ozone treated ITO substrates from organic films should be considered for enhancing stabilities of typical semiconducting organic films.

2.4. Stability Enhancement in Rubrene-Based OPV Devices

To further consolidate our discussions on film stability and thus the device reliability, rubrene-based OPV devices were fabricated

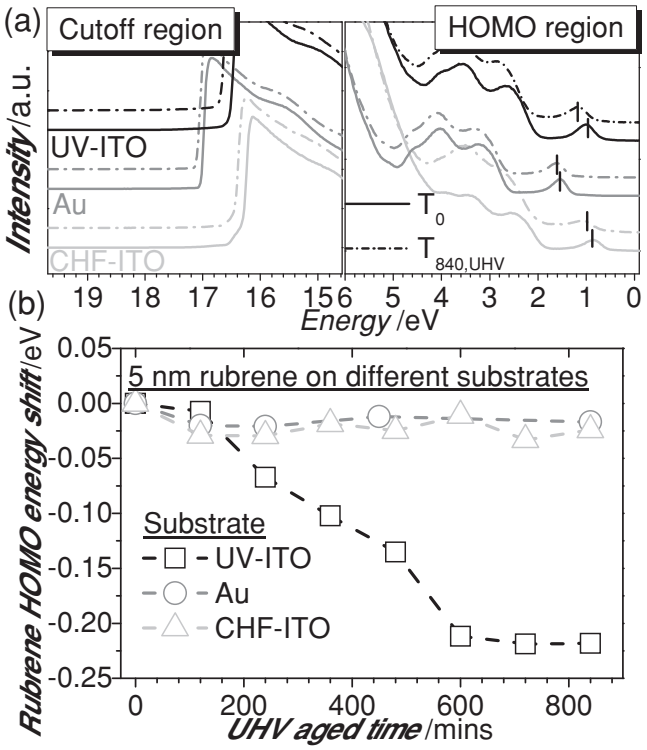

Figure 4. a) UPS He-Iα spectra of rubrene films prepared on UV-ITO (top), Au (middle), and CHF-ITO (bottom) substrates before (solid line) and after 840 min aging (solid-dotted) in UHV condition. b) Energy shifts in the HOMO level of rubrene prepared on UV-ITO (□), Au (○), and CHF-ITO (△) substrates aging in UHV conditions.

on UV-ITO (UV-ITO device), ITO/Au (Au-ITO device), and ITO/CHF (CHF-ITO device) substrates. The device configurations are: anode substrate/rubrene (35 nm)/C_{60} (45 nm)/BCP (5 nm)/Al. Encapsulated devices were illuminated by 100 mW/cm^2 solar simulated irradiation continuously for 150 min.

Figure 5 compares degradation rates of the three devices. The power conversion efficiency (PCE) and open circuit voltage (V_{oc}) are normalized to their corresponding initial values for better comparison while their absolute values are summarized in **Table 2**. Performance of a CuPc/C_{60} reference device with a configuration of UV-ITO/CuPc (35 nm)/C_{60} (45 nm)/BCP (5 nm)/Al was also included for comparison. Performance of the reference device showed negligible degradation over the testing period. This suggests that the employed encapsulation

Table 1. Valence parameters of rubrene prepared on different substrates obtained by UPS studies before and after 840 min aging.

	Work function [eV]		HOMO edge w.r.t. Fermi level [eV]	
	T_0	$T_{840,UHV}$	T_0	$T_{840,UHV}$
UV-ITO/rubrene	4.7	4.5	0.6	0.8
Au/rubrene	4.2	4.1	1.3	1.3
CHF-ITO/rubrene	4.8	4.7	0.6	0.6

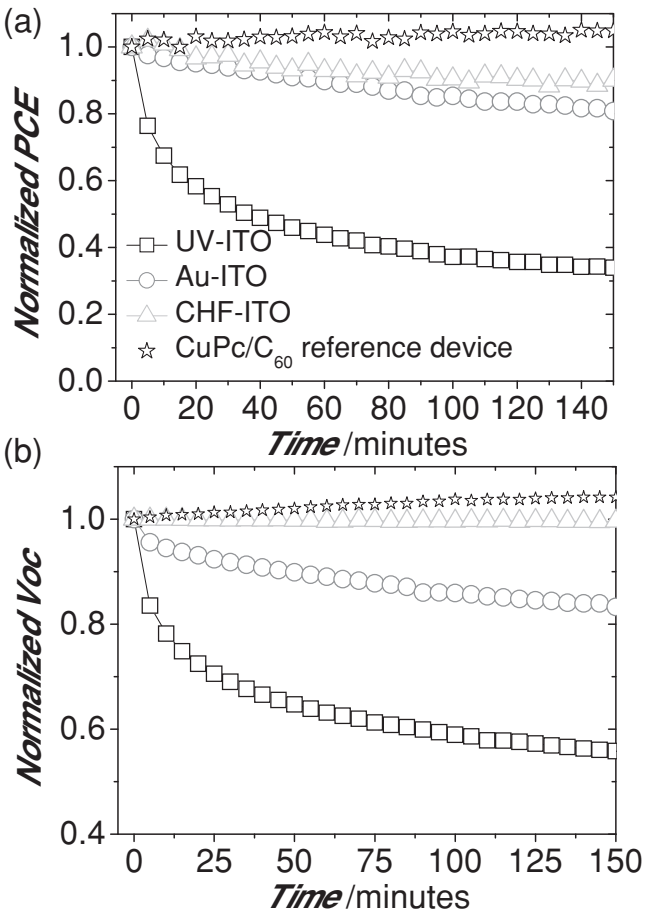

Figure 5. Photovoltaic responses showing the normalized a) PCE and b) V_{oc} of encapsulated UV-ITO device (□), Au-ITO device (○), CHF-ITO device (△), and CuPc/C60 reference device (☆) during 150 min continuous 1 Sun AM1.5G illumination.

scheme does provide enough protection to the device against degradation caused by the atmospheric surroundings.[28,29]

Consistent with the photoemission results, PCE and V_{oc} of the UV-ITO device rapidly dropped to 40 and 50% of their initial values, respectively, after 150 min of continuous illumination. Noteworthy, upon isolation of ITO interface, much less losses in PCE were observed in both the Au-ITO and the CHF-ITO devices. More importantly, a very high V_{oc} of 0.92 V is maintain in the CHF-ITO device throughout the test (see Table 2). These OPV device performances further consolidate our discussions on the UV-ITO induced organic film/device degradation. Upon the ITO-induced aging, carrier trap states are induced by oxygen near the HOMO of the rubrene (see Figure 3). These new trap states can act as recombination centers for photo-induced excitons and thus degrade charge generation at the rubrene/C_{60} interface and result in deteriorated photovoltaic response.

It should be pointed out that for fair stability comparison, the thicknesses of active layers in the CHF-ITO device shown in Figure 5 have not been fully optimized. The experimental results for optimized devices are shown in Figure S2 and Table SI in the Supporting Information. A similar stability enhancement was observed for the optimized devices after 150 min continuous illumination. More importantly, the PCE of the optimized CHF-ITO device can reach 2.5–2.9% over the measurement duration. This performance is much higher than that reported recently in standard CuPc/C_{60} devices.[30–32]

3. Conclusion

While UV-ITO have been widely used in organic electronic devices, we here showed that they can cause PL degradation of common organic semiconductors such as NPB, Alq_3, and rubrene. The degradation would be further accelerated with illumination. UPS and XPS studies show that reactive surface oxygen species generated upon UV-ozone treatment is the major cause for the degradation of rubrene film deposited on ITO substrate. The reactive oxygen species on the UV-ITO induce a gap-state in the energy gap of rubrene and shifting its HOMO away from the Fermi level. The observations were further supported by performance data of rubrene-based OPV devices. This work suggests that commonly used ITO-coated glass with UV-ozone treatment has far-reaching implications for device stability.

4. Experimental Section

Device Fabrication and PL Measurements: Patterned ITO coated glass substrates with a sheet resistance of 30 Ω/square were routinely cleaned with Decon 90, rinsed using deionized water, and dried in an oven for at least 2 h. This as-cleaned ITO (AC-ITO) glasses were then treated

Table 2. The photoresponse of OPV devices with rubrene (35 nm)/C_{60} (45 nm)/BCP (5 nm)/Al deposited on i) UV-ITO (UV-ITO device); ii) ITO/Au (5 nm) (Au-ITO device); and iii) ITO/CHF (1.5 nm) (CHF-ITO devices) substrates before and after 150 min of continuous illumination. The photoresponse of the reference device with CuPc (35 nm)/C_{60} (45 nm)/BCP (5 nm)/Al deposited on UV-ITO substrate (CuPc/C_{60} reference device) is also included.

Devices	V_{oc} [V]		J_{sc}[a] [mA/cm^2]		FF[b]		PCE [%]	
	T_0	$T_{150,1sun}$	T_0	$T_{150,1sun}$	T_0	$T_{150,1sun}$	T_0	$T_{150,1sun}$
i) UV-ITO device	0.88	0.49	3.6	2.8	0.46	0.35	1.4	0.5
ii) AU-ITO device	0.76	0.63	0.8	0.8	0.35	0.34	0.2	0.2
iii) CHF-ITO device	0.92	0.92	4.2	3.9	0.6	0.56	2.3	2.0
iv) CuPc/C_{60} reference device	0.46	0.48	5.9	5.8	0.55	0.57	1.5	1.6

[a]Short-circuit current density; [b]Fill factor.

with ultraviolet-ozone (UV-ITO). Some UV-ITO substrates were further treated with a CHF_3 plasmas (CHF-ITO) or coated with a 5 nm gold film (Au-ITO) prior to device fabrication.[23]

For device fabrication, all organic and metal thin films are prepared by thermal evaporation. Deposition rates of organic films were monitored with a quartz oscillating crystal and controlled at 0.1–0.2 nm/s. After deposition of the organic layers, an Al cathode (80 nm) was deposited by thermal evaporation through a shadow mask. The measured active devices areas were 0.12 cm^2. All devices were measured after encapsulation in a nitrogen-filled glove box immediately after cathode deposition. Current–voltage (*J–V*) characteristics were measured with a programmable Keithley model 237 power source. Device characteristics were measured under illumination with an intensity of 100 mW/cm^2 from an Oriel 150 W solar simulator with AM1.5G (AM: air mass, G: global) filters.

For PL measurement, 50 nm thick NPB, Alq3, rubrene films were thermally deposited on quartz, AC-ITO, and UV-ITO glass substrates at a controlled rate of 0.1–0.2 nm/s. PL spectra of the as-prepared samples were recorded using a Perkin-Elmer LS50B luminescence spectrophotometer. The samples were irradiated continuously with AM1.5G simulated solar illumination at 100 mW/cm^2 intensity for 40 minutes.

Photoelectron Spectroscopy: All photoelectron spectroscopies were carried out with a VG ESCALAB 220i-XL surface analysis system equipped with a He-discharge lamp providing He-I photons of 21.22 eV for UPS analysis; and a monochromatic Al-Kα X-ray gun with photons energies of 1486.6 eV for XPS investigation.[33] The base vacuum of the system is $\approx 10^{-10}$ Torr. All organic films were thermally evaporated on UV-ITO glass or sputter-cleaned Au or CHF-ITO substrates inside the deposition chamber at a pressure of $\approx 2 \times 10^{-9}$ Torr. The freshly deposited films were transferred to the analysis chamber for UPS and XPS measurements without vacuum break. UPS He I measurements were performed to study the valence states of the prepared films. Vacuum level offsets were obtained from the shifts of the intensity thresholds at the lowest inelastic electrons kinetic energy cut-off, with a bias of –5.0 V with respect to ground. The position of the Fermi edge was calibrated using a clean Au film, and all spectra presented were plotted with respect to the determined Fermi level. All XPS measurements were calibrated with reference to the $4f_{7/2}$ core level (83.98 eV) of a freshly sputtered Au film. Positions of the LUMO levels of rubrene and C_{60} were estimated according to the charge transport gaps reported by measurements using inverse photoelectron spectroscopy.[34,35]

Supporting Information

Supporting Information is available from the Wiley Online Library or from the author.

Acknowledgements

The work described in this paper was supported by a grant from the Research Grants Council of the Hong Kong Special Administrative Region, China (Project No. T23-713/11).

Received: July 27, 2012
Published online: October 23, 2012

[1] C. W. Tang, *Appl. Phys. Lett.* **1986**, *48*, 183.
[2] M. Cai, Z. Ye, T. Xiao, R. Liu, Y. Chen, R. W. Mayer, R. Biswas, K. Ho, R. Shinar, J. Shinar, *Adv. Mater.* **2012**, *24*, 4337.
[3] Z. Shen, P. E. Burrows, V. Bulović, S. R. Forrest, M. E. Thompson, *Science* **1997**, *276*, 2009.
[4] Y. Kuwabara, H. Ogawa, H. Inada, N. Noma, Y. Shirota, *Adv. Mater.* **1994**, *6*, 677.
[5] M. Cai, T. Xiao, E. Hellerich, Y. Chen, R. Shinar, J. Shinar, *Adv. Mater.* **2011**, *23*, 3590.
[6] Y. Shirota, *J. Mater. Chem.* **2000**, *10*, 1.
[7] H. J. Kim, J. W. Kim, H. H. Lee, B. Lee, J. Kim, *Adv. Funct. Mater.* **2012**. *22*, 4244.
[8] S. T. Lee, Z. Q. Gao, L. S. Hung, *Appl. Phys. Lett.* **1999**, *75*, 1404.
[9] Y. Qiu, Y. Gao, L. Wang, D. Zhang, *Synth. Met.* **2002**, *130*, 235.
[10] C. C. Wu, C. I. Wu, J. C. Sturm, A. Kahn, *Appl. Phys. Lett.* **1997**, *70*, 1348.
[11] H. Aziz, Z. Popovic, *Chem. Mater.* **2004**, *16*, 4522.
[12] F. So, D. Kondakov, *Adv Mater.* **2010**, *22*, 3762.
[13] L. Hung, C. Chen, *Mater. Sci. Eng. R-Rep.* **2002**, *39*, 143.
[14] M. Jorgensen, K. Norrman, S. A. Gevorgyan, T. Tromholt, B. Andreasen, F. C. Krebs, *Adv. Mater.* **2012**, *24*, 580.
[15] J. X. Tang, Y. Q. Li, X. Dong, S. D. Wang, C. S. Lee, L. S. Hung, S. T. Lee, *Appl. Surf. Sci.* **2004**, *239*, 117.
[16] H. Lu, M. Yokoyama, *J. Cryst. Growth* **2004**, *260*, 186.
[17] D. J. Milliron, I. G. Hill, C. Shen, A. Kahn, J. Schwartz, *J. Appl. Phys.* **2000**, *87*, 572.
[18] J. Moon, J. Bae, J. Jeong, S. Jeong, N. Park, H. Kim, *Appl. Phys. Lett.* **2007**, *90*, 163516.
[19] M. G. Helander, Z. B. Wang, J. Qiu, M. T. Greiner, D. P. Puzzo, Z. W. Liu, Z. H. Lu, *Science* **2011**, *332*, 944.
[20] J. Olivier, B. Servet, M. Vergnolle, M. Mosca, G. Garry, *Synth. Met.* **2001**, *122*, 87.
[21] Z. H. Huang, X. T. Zeng, X. Y. Sun, E. T. Kang, J. Y. H. Fuh, L. Lu, *Org. Electron.* **2008**, *9*, 51.
[22] H. Aziz, Z. D. Popovic, N. Hu, A. Hor, G. Xu, *Science* **1999**, *283*, 1900.
[23] M. F. Lo, T. W. Ng, S. L. Lai, M. K. Fung, S. T. Lee, C. S. Lee, *Appl. Phys. Lett.* **2011**, *99*, 033302.
[24] T. W. Ng, M. F. Lo, Y. C. Zhou, Z. T. Liu, C. S. Lee, O. Kwon, S. T. Lee, *Appl. Phys. Lett.* **2009**, *94*, 193304.
[25] Y. Tanaka, K. Kanai, Y. Ouchi, K. Seki, *Chem. Phys. Lett.* **2007**, *441*, 63.
[26] M. Kytka, A. Gerlach, F. Schreiber, J. Kovac, *Appl. Phys. Lett.* **2007**, *90*, 131911.
[27] L. S. Liao, L. F. Cheng, M. K. Fung, C. S. Lee, S. T. Lee, M. Inbasekaran, E. P. Woo, W. W. Wu, *Phys. Rev. B* **2000**, *62*, 10004.
[28] M. Jørgensen, K. Norrman, F. C. Krebs, *Sol. Energy Mater. Sol. Cells* **2008**, *92*, 686.
[29] M. F. Lo, T. W. Ng, S. L. Lai, F. L. Wong, M. K. Fung, S. T. Lee, C. S. Lee, *Appl. Phys. Lett.* **2010**, *97*, 143304.
[30] M. D. Perez, C. Borek, P. I. Djurovich, E. I. Mayo, R. R. Lunt, S. R. Forrest, M. E. Thompson, *Adv. Mater.* **2009**, *21*, 1517.
[31] K. S. Yook, B. D. Chin, J. Y. Lee, B. E. Lassiter, S. R. Forrest, *Appl. Phys. Lett.* **2011**, *99*, 043308.
[32] W. Jeong, Y. E. Lee, H. Shim, T. Kim, S. Kim, J. Kim, *Adv. Funct. Mater.* **2012**, *22*, 3089.
[33] T. W. Ng, M. F. Lo, Q. D. Yang, M. K. Fung, C. S. Lee, *Adv. Funct. Mater.* **2012**, *22*, 3035.
[34] H. Ding, Y. Gao, *Appl. Phys. A* **2009**, *95*, 89.
[35] R. W. Lof, M. A. Vanveenendaal, B. Koopmans, H. T. Jonkman, G. A. Sawatzky, *Phys. Rev. Lett.* **1992**, *68*, 3924.